General Disclaimer

One or more of the Following Statements may affect this Document

- This document has been reproduced from the best copy furnished by the organizational source. It is being released in the interest of making available as much information as possible.

- This document may contain data, which exceeds the sheet parameters. It was furnished in this condition by the organizational source and is the best copy available.

- This document may contain tone-on-tone or color graphs, charts and/or pictures, which have been reproduced in black and white.

- This document is paginated as submitted by the original source.

- Portions of this document are not fully legible due to the historical nature of some of the material. However, it is the best reproduction available from the original submission.

X-692-77-90

PREPRINT

TMX 71319

INTERPLANETARY BASELINE OBSERVATIONS OF TYPE III SOLAR RADIO BURSTS

R. R. WEBER
R. J. FITZENREITER
J. C. NOVACO
J. FAINBERG

APRIL 1977

GSFC — GODDARD SPACE FLIGHT CENTER —
GREENBELT, MARYLAND

INTERPLANETARY BASELINE OBSERVATIONS OF TYPE III SOLAR RADIO BURSTS

R. R. Weber
R. J. Fitzenreiter
J. C. Novaco
J. Fainberg
NASA/Goddard Space Flight Center
Laboratory for Extraterrestrial Physics
Greenbelt, MD 20771

ABSTRACT

The first simultaneous observations of type III radio bursts using spacecraft separated by several tenths of an AU have been made using the solar orbiters HELIOS-A and -B. The burst beginning at 1922 UT on March 28, 1976, has been located from the intersection of the source directions measured at each spacecraft, and from the burst arrival time differences. Wide baseline observations give the radial distance of the source at each observing frequency. Consequently, coronal electron densities and exciter velocity were determined directly, without the need to assume a density model as has been done with single spacecraft observations. The separation of HELIOS-A and -B has also provided the first measurements of burst directivity at low frequencies. For the March 28 burst the intensity observed from near the source longitude (HELIOS-B) was significantly greater than from 60^{o} W of the source (HELIOS-A).

INTRODUCTION

Past observations of low frequency (25-5000 kHz) type III solar radio bursts by single spinning spacecraft have measured burst directions in the spacecraft equatorial plane (e.g., Fainberg et al., 1972). Simultaneous observations by two near-Earth spacecraft spinning in different planes have measured burst directions both in and out of the ecliptic (Baumback et al., 1975; Fitzenreiter et al., 1977). HELIOS-A and HELIOS-B, launched into solar orbits in December 1974 and January 1976, respectively, provide the first opportunity for low frequency observations from widely separated spacecraft. The separation of these two spinning spacecraft (typically 0.3 AU) allows the burst to be located by triangulation, thereby adding information on the radial distance of the source which was not available from previous measurements.

Each HELIOS spacecraft is in a solar ecliptic orbit having an aphelion of 1.0 AU, perihelion of 0.3 AU, and sidereal period of six months. The low frequency radio astronomy experiment employs two extendable 15-m booms forming an electric dipole which lies in the equatorial plane of the spacecraft. The spin axis is normal to the ecliptic and the spin period is one second. A high-impedance preamplifier located at the root of each boom connects to the 16-channel radiometer operating over the frequency range of 26-3000 kHz with a channel bandwidth of 10 kHz and dynamic range of 90 dB. Data collection is spin-synchronous, with each frequency operating for sixteen samples (one-half spin). This sequence allows source direction-finding for every one-half second of data. Failure of a HELIOS-A antenna mechanism caused one boom to be shorted to the spacecraft, thereby degrading the sensitivity for that experiment.

In all other respects the radio astronomy experiments performed as planned. A more detailed experiment description has been presented by Weber (1975).

Simultaneous observations with a long baseline allow measurements of type III burst source locations in the ecliptic by two independent means. One method involves the difference in propagation path length from the source to the two spacecraft, determined from the difference in burst arrival times. For a given event the difference in path length defines a hyperboloid on which the source lies. Figure 1 shows hyperbolae of constant time difference in the ecliptic for HELIOS-A and -B on March 28, 1976. The third dimension may be obtained by rotating these curves about the axis containing the two spacecraft. When the source is near the ecliptic and remote from both spacecraft, the curves shown in Figure 1 can be used directly to obtain the locus of possible source positions.

Triangulation by direction finding is the other means of locating the source of a type III burst. The phase of the spin modulation in the radiation observed by a spinning spacecraft defines a plane containing the spin axis and the source centroid. With two spinning spacecraft observing over a long baseline, the intersection of the planes determined by each spacecraft gives a line containing the source. For HELIOS-A and -B this line is normal to the ecliptic, so the projection of the source location on the ecliptic is completely determined. If the burst exciter remains within the latitude range of the active centers on the Sun, i.e., within approximately 30 degrees of the solar equator, then the difference between the actual radial distance to the source and its measured projection on the ecliptic is less than ~15 percent. Consequently, the

speed of the exciter and the electron density along the exciter path may both be obtained from observations of a type III burst at a number of frequencies. Previously, measurements of individual bursts from a single observing position required that either the exciter speed or density scale be assumed in order to obtain the other from the data (Fainberg et al., 1972).

In addition to locating the source of a burst, long baseline observations give a measurement of burst directivity by comparing the intensities obtained simultaneously at different solar longitudes. HELIOS-A and -B have provided the first comparisons of relative intensity at different observing directions for low frequency bursts.

As an example of the new observing techniques made possible by an extended baseline, joint HELIOS-A and -B measurements of the type III solar burst occurring near 1930 UT on March 28, 1976 are presented. In the next section we analyze the arrival time differences and burst directions, followed by comparison of observed intensities at the two spacecraft positions.

SOURCE LOCATION

Intensity-time profiles from both HELIOS-A and -B show that the March 28 type III burst is complex and that the profile shape is independent of viewing direction. The burst contains several components, corresponding to several distinct exciters. In order to find the source loci from arrival time differences, accurate measurements of the peak times are needed at both HELIOS-A and -B for each component; therefore the profiles were decomposed into component bursts as shown in Figure 2. The shape of the components was modeled after numerous simple bursts observed previously by RAE-1 and IMP-6. A least-squares fit to the HELIOS data allowed for intensity (vertical) and time (horizontal) shifts of the several components. The curves passing through the data show that the sum of the component bursts is a good fit to the data points. The best fit was obtained using four components over most of the frequency range.

The times of the peaks of the fitted components are plotted in Figure 3 for both spacecraft, along with uncertainties in peak time obtained from the least-squares residuals. Note that the time between the component peaks at a given spacecraft is nearly equal for all frequencies, which indicates that the corresponding exciters have approximately the same speed. This supports the interpretation that this profile shape is composed of several distinct bursts.

Burst locations obtained from direction finding and from arrival time differences are given in Figure 4 for 1010, 1320, and 2280 kHz. The burst centroid, averaged over the two strongest components of the burst, is found from the intersections of the measured directions at HELIOS-A and -B. The extent of the box around the point of intersection includes

uncertainties in measuring the burst arrival directions and fluctuations in the centroid position over the burst duration.

The burst time differences have been used with the computed source loci, as in Figure 1, to obtain the locus of possible source positions. The range of loci shown in Figure 4 arises from uncertainties in measuring burst peak times at both spacecraft. The burst locations determined by direction finding and time differences are in good agreement. Uncertainties in burst centroid position for this event are ± 0.01 AU in radial distance from the Sun and $\pm 12^{0}$ in solar longitude.

A ray trace analysis is underway in this laboratory to study propagation effects on low frequency type III burst observations. Initial results indicate that for this event scattering and refractive effects on burst arrival directions at the two spacecraft are within the uncertainties shown in Figure 4. Measured arrival time differences at the two spacecraft have been corrected by 5-10 seconds to allow for propagation path differences resulting from longitude-dependent scattering effects. Preliminary analysis shows that rays observed at the limb (as seen from HELIOS-A) are delayed more than rays observed near central meridian (as seen from HELIOS-B).

In addition to the HELIOS-A and -B data, this burst was observed by the Radio Astronomy Explorer-2 (RAE-2), which is in lunar orbit. RAE-2 is described by Alexander et al. (1975). Unfortunately, the data from RAE-2 are saturated at the burst peak, due to the higher sensitivity of the longer antennas. Nevertheless, matching the rise and fall of the RAE-2 burst profile with the HELIOS-A observations provides further confirmation of the burst locations, as shown in Figure 4.

CORONAL DENSITY

A flare associated with this event occurred at 1912 UT at heliocentric coordinates 7^{o} S, 28^{o} E. Average positions of the two strongest burst components range from 10^{o} E - 30^{o} E longitude, somewhat west of the flare site. The observed distance from the Sun to each emission level is used to derive the electron density along the burst trajectory, as shown in Figure 5. Electron density at each source distance was obtained assuming the emission occurs at twice the local plasma frequency (see Lin et al., 1973). The distance scale is based on the ecliptic projection of the burst positions. If the burst trajectory remains near the ecliptic then the projection errors are negligible. These data are compared with the equatorial electron density model of Newkirk (1967) in Figure 5. Both the model and the data for this event correspond to minimum sunspot conditions, and there appears to be good agreement. An extrapolation of the RAE-1 density scale (Fainberg and Stone, 1971) to coronal levels below 0.1 AU yields electron densities which are a factor of 4 higher than those in Figure 5. The RAE-1 scale, however, was obtained during solar maximum, when densities at these coronal levels can be expected to be at least a factor ~2 larger than at solar minimum (Newkirk, 1967).

EXCITER SPEED

Simultaneous measurements of the energy spectrum of solar electrons and type III radio bursts have shown that the exciter electrons are dispersed in velocity (Lin et al., 1973). The onset and gradual rise of the burst profile are due to the arrival of the fastest electrons at the source region, which are followed by more numerous, less energetic electrons. Thus, the burst peak corresponds to the passage of slower electrons through the emission regions. Burst position for the March 28 event is plotted as a function of burst peak time in Figure 6, from which the exciter speed may be obtained directly. The speed of the slower exciter electrons, given by the slope of the straight line fitted through the data, is $v/c = 0.13 \pm 0.03$, where c is the speed of light in vacuum. Other measurements have obtained exciter speeds between 0.1c - 0.2c for burst peaks (Fainberg et al., 1972; Lin et al., 1973).

APPARENT BURST DIRECTIVITY

These observations provide the first amplitude measurements of a low frequency burst from two quite different viewing directions. As shown in Figure 4, HELIOS-B is within 20^{o} of the source heliocentric longitude, whereas HELIOS-A is more than 70^{o} away from the source. Thus the longitude dependence of observed intensity, due to coronal propagation effects and possible intrinsic source directivity, can be measured.

The intensity at HELIOS-A relative to the intensity at HELIOS-B is plotted in Figure 7. The frequency scale is along the upper horizontal axis and the corresponding angle θ, which is the difference in observing direction from the two spacecraft to the source region, is along the lower horizontal scale. Relative intensity at each spacecraft has been adjusted for its distance to the source, as well as for a 6 dB loss at HELIOS-A due to one shorted antenna boom. Even with these corrections, the data show that the intensity at HELIOS-A is lower than at HELIOS-B by an amount which varies from 3 to 9 dB as θ increases from approximately 60^{o} to 70^{o}. Below 585 kHz, corresponding to $\theta > 70^{o}$, the burst was not observed at HELIOS-A due to lower sensitivity and to the lower burst intensity. HELIOS-B, however, observed the burst down to 50 kHz. Thus, radiation was gradually cut off in the direction of HELIOS-A as the source moved toward the radio limb until, below 585 kHz, it was not detected at HELIOS-A. The value at 3000 kHz was an exception to the systematic variation of intensity with θ. However, the 3000 kHz burst longitude was $\sim 20^{o}$ farther east than the other frequencies and is consequently closer to the radio limb as seen by HELIOS-A.

An intensity variation with observing angle was also found for type III burst limb events at 169 MHz by the STEREO-1 experiment using a Mars planetary probe together with ground-based observations (Caroubalous et al., 1974). In that experiment the ratio of intensities of individual bursts measured simultaneously in two directions was found to increase from 3 to 10 dB as the source longitude increased, which is the same range of relative intensities shown in Figure 8. It is noteworthy that the burst radiation patterns seen by HELIOS and STEREO are similar at frequencies two orders of magnitude apart, since 169 MHz radiation is generated close to the solar surface, where density gradients and inhomogeneites are quite different. This similarity suggests that the burst radiation pattern may not be very sensitive to these parameters.

SUMMARY

The wide separation of the HELIOS-A and -B solar orbiters permits new types of measurements of low frequency radio bursts. This paper has described multi-satellite analysis techniques and has presented observations of a complex solar burst on March 28, 1976. Two-spacecraft observations of this burst were obtained in the frequency range 3000 - 585 kHz. The heliocentric coordinates of the burst trajectory and the speed of the exciter have been obtained from the arrival directions and times measured at each spacecraft. Burst directivity was measured and found to be similar to the only other comparable measurements, at 169 MHz.

The portion of the burst trajectory observed by both spacecraft covered the heliocentric distances 0.03 - 0.1 AU. This is an important area of the heliosphere for study because acceleration of the solar wind occurs in this region. Type III solar bursts have the unique capability of providing information on two solar wind parameters, the electron density variation and magnetic field configuration, practically instantaneously over a wide range of solar distances. For this burst, the electron density along the trajectory agrees with the Newkirk (1967) model for equatorial electron density at solar minimum. The longitude of the burst source was approximately 20^{o} west of the initiating flare, suggesting non-radial magnetic field lines connecting back to the flare site. Before generalizations can be made, however, many such events must be observed and analyzed taking propagation effects into account. Multi-spacecraft observations, combined with data on surface features on the Sun, may then be able to provide information on solar wind structure in the vicinity of active regions.

REFERENCES:

1. Alexander, J. K., Kaiser, M. L., Novaco, J. C., Grena, F. R., and Weber, R. R.: 1975, Astron. & Astrophys., 40, 365.
2. Baumback, M. M., Kurth, W. S., and Gurnett, D. A.: 1976, Solar Phys., 48, 361.
3. Caroubalos, C., Poquerusse, M., and Steinberg, J. L.: 1974, Astron. and Astrophys., 32, 255.
4. Fainberg, J. and Stone, R. G.: 1971, Solar Phys., 17, 392.
5. Fainberg, J., Evans, L. G., and Stone, R. G.: 1972, Science, 178, 743.
6. Fitzenreiter, R. J., Fainberg, J., Weber, R. R., Alvarez, H., Haddock, F. T., and Potter, W. H.: 1977, Solar Phys., May 1977.
7. Lin, R. P., Evans, L. G., and Fainberg, J.: 1973, Astrophys. Letts., 14, 191.
8. Newkirk, G.: 1967, Ann. Rev. of Astr. and Astrophys., 5, 213.
9. Riddle, A. C.: 1974, Solar Phys., 35, 153.
10. Weber, R. R.: 1975, Raumfahrtforschung, 19, 250.

FIGURE CAPTIONS

Figure 1 Source loci for time differences observed by HELIOS-A and -B on March 28, 1976. For example, source on the 90 sec locus will arrive at HELIOS-A 90 sec earlier than at HELIOS-B. The Earth is off the bottom of the figure.

Figure 2 Complex burst observed by HELIOS-A and -B. The burst profile has been fitted by a model which is the sum of four components.

Figure 3 Observed arrival times for peaks of burst components observed by HELIOS-A and -B. Components A3 and A4 (see Figure 2) were too weak to provide reliable times.

Figure 4 Location of burst source regions given by the intersections of the directions measured at HELIOS-A and -B, and by arrival time differences at HELIOS-A and -B as well as HELIOS-A and RAE-2. Direction finding and arrival time results are in agreement.

Figure 5 Electron density determined for the March 28 burst trajectory, using the measured source locations at each observing frequency and assuming emission occurs at twice the local plasma frequency. The Newkirk (1967) electron density model is shown for comparison.

Figure 6 Burst exciter speed determined for the March 28 event from the observed burst peak times and positions.

Figure 7 Burst intensity observed at HELIOS-A compared to HELIOS-B for different frequencies. θ is the angle between HELIOS-A and -B, measured from the source location. Consequently these data are a measure of the radiation pattern for the burst in the interplanetary medium.

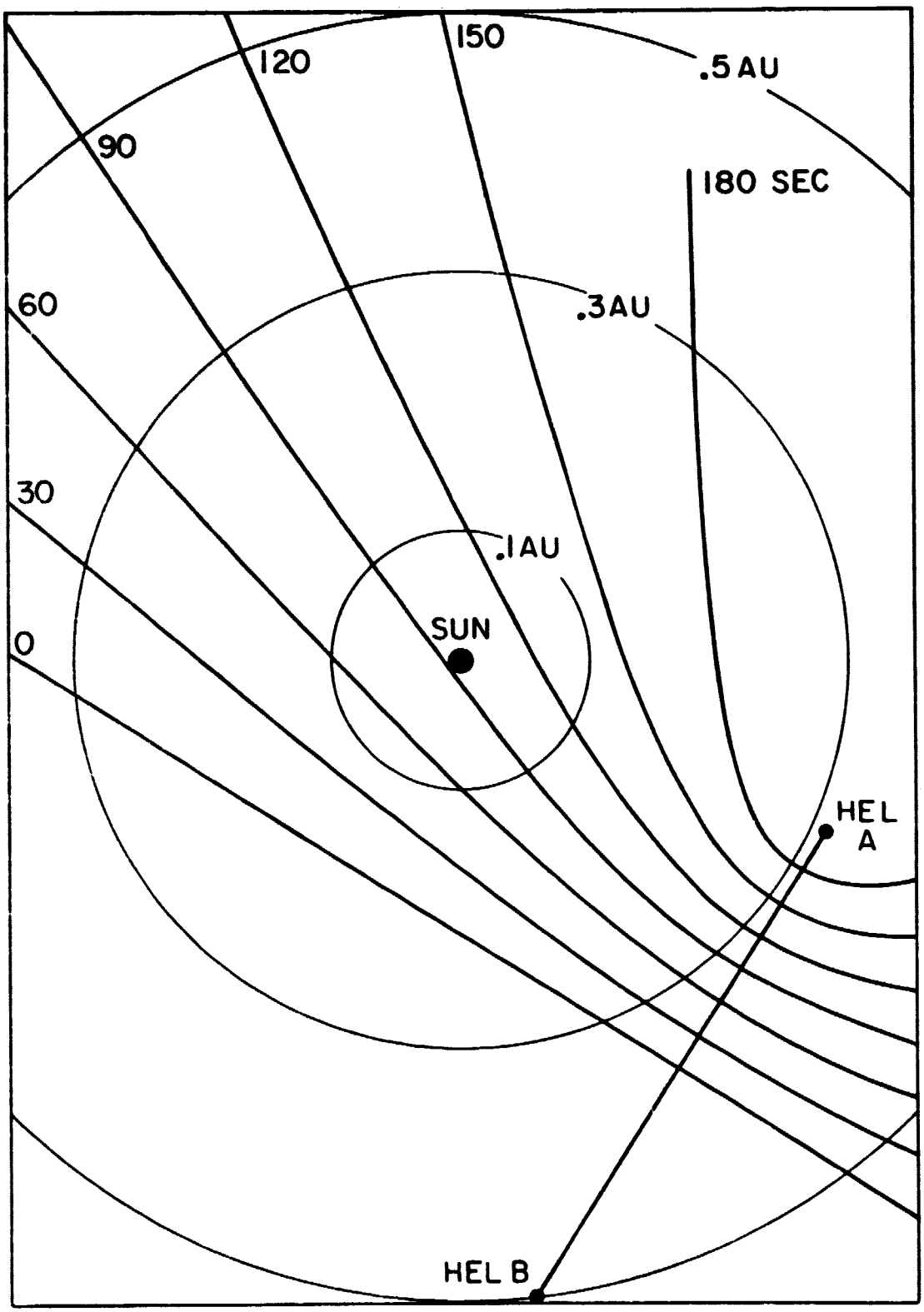

Figure 1

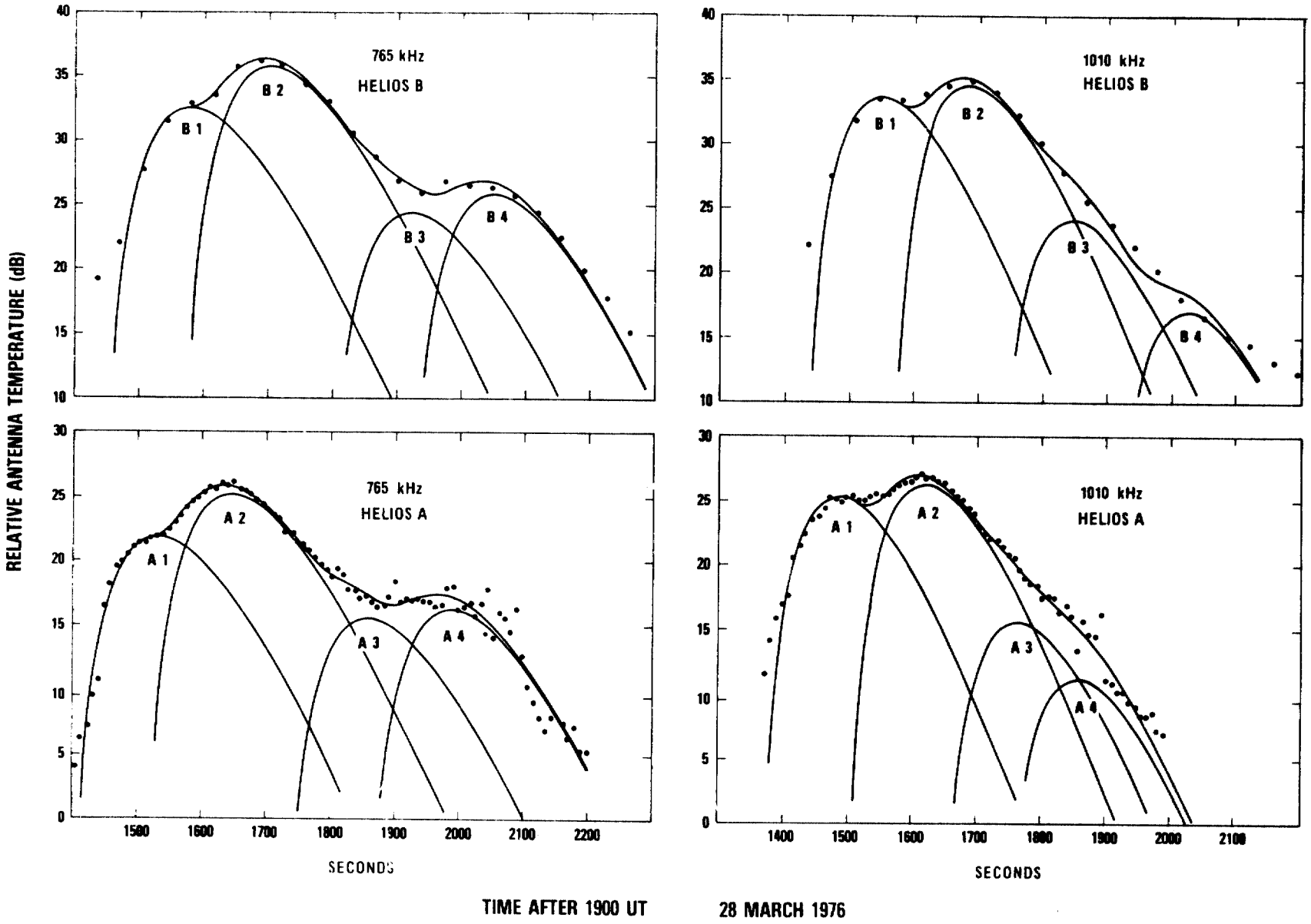
765 kHz
HELIOS B
B 1
B 2
B 3
B 4
1010 kHz
HELIOS B
B 1
B 2
B 3
B 4
765 kHz
HELIOS A
A 1
A 2
A 3
A 4
1010 kHz
HELIOS A
A 1
A 2
A 3
A 4
RELATIVE ANTENNA TEMPERATURE (dB)
SECONDS
SECONDS
TIME AFTER 1900 UT
28 MARCH 1976

Figure 2

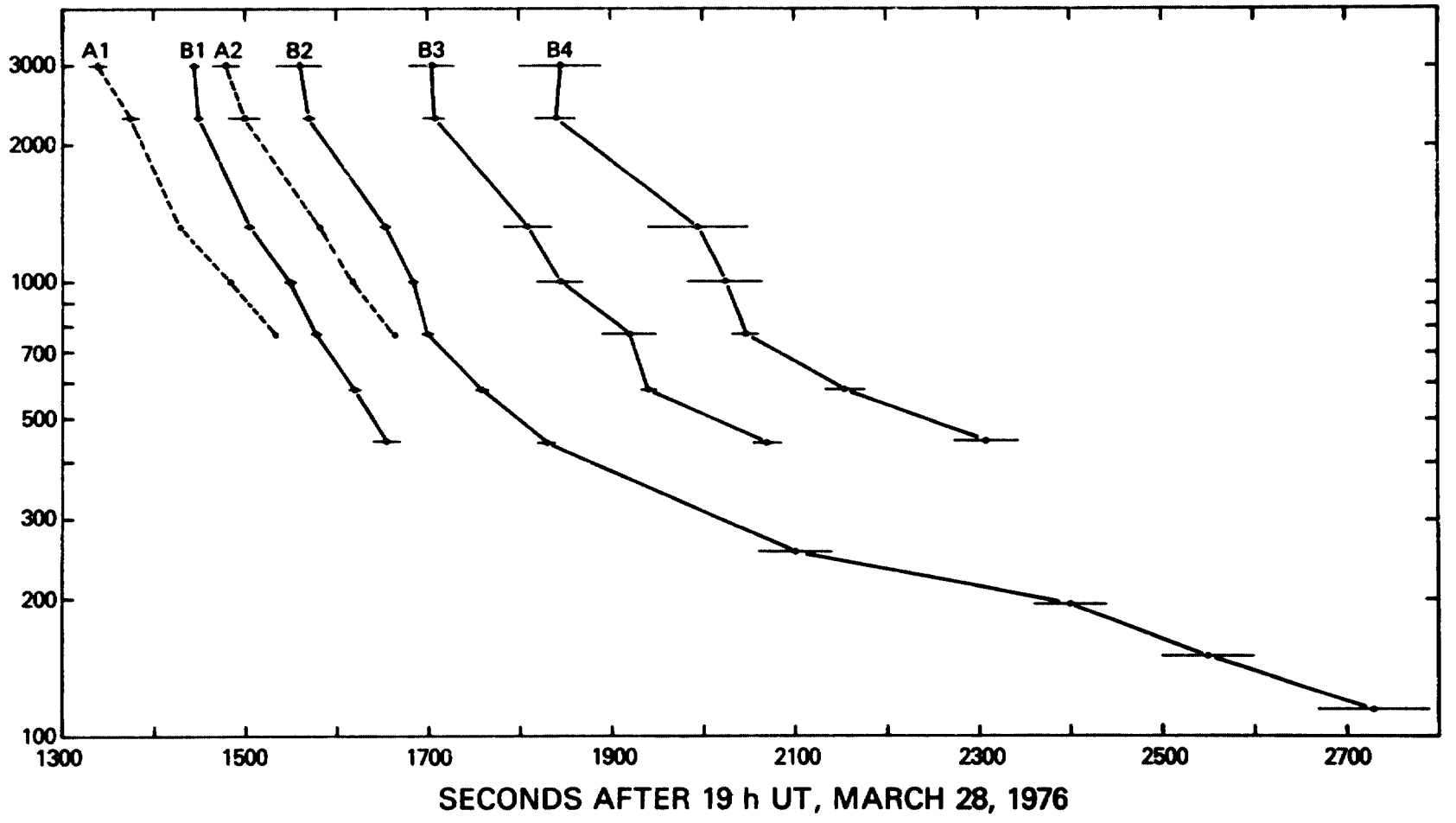
A1
B1
A2
B2
B3
B4
3000
2000
1000
700
500
300
200
100
1300
1500
1700
1900
2100
2300
2500
2700
SECONDS AFTER 19 h UT, MARCH 28, 1976

Figure 3

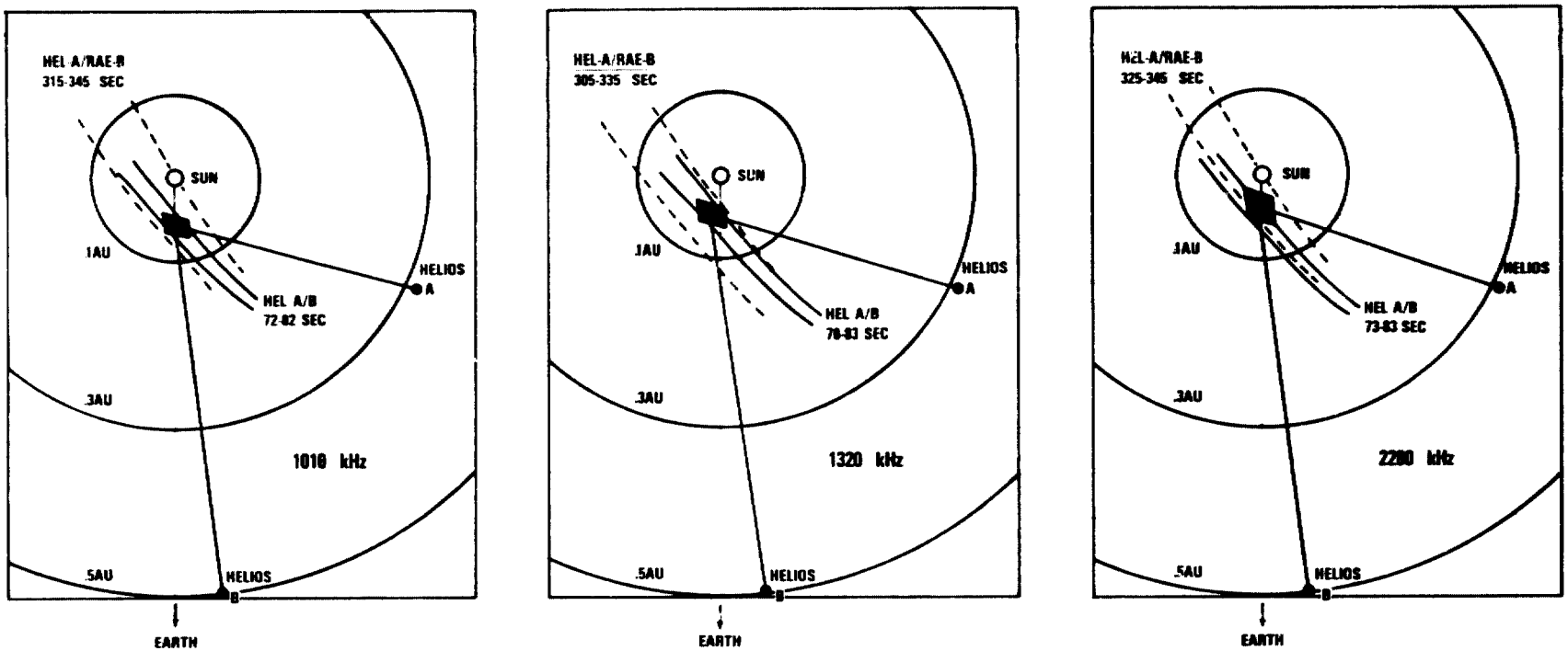

SOLAR BURST LOCATIONS 28 MARCH 1976

Figure 4

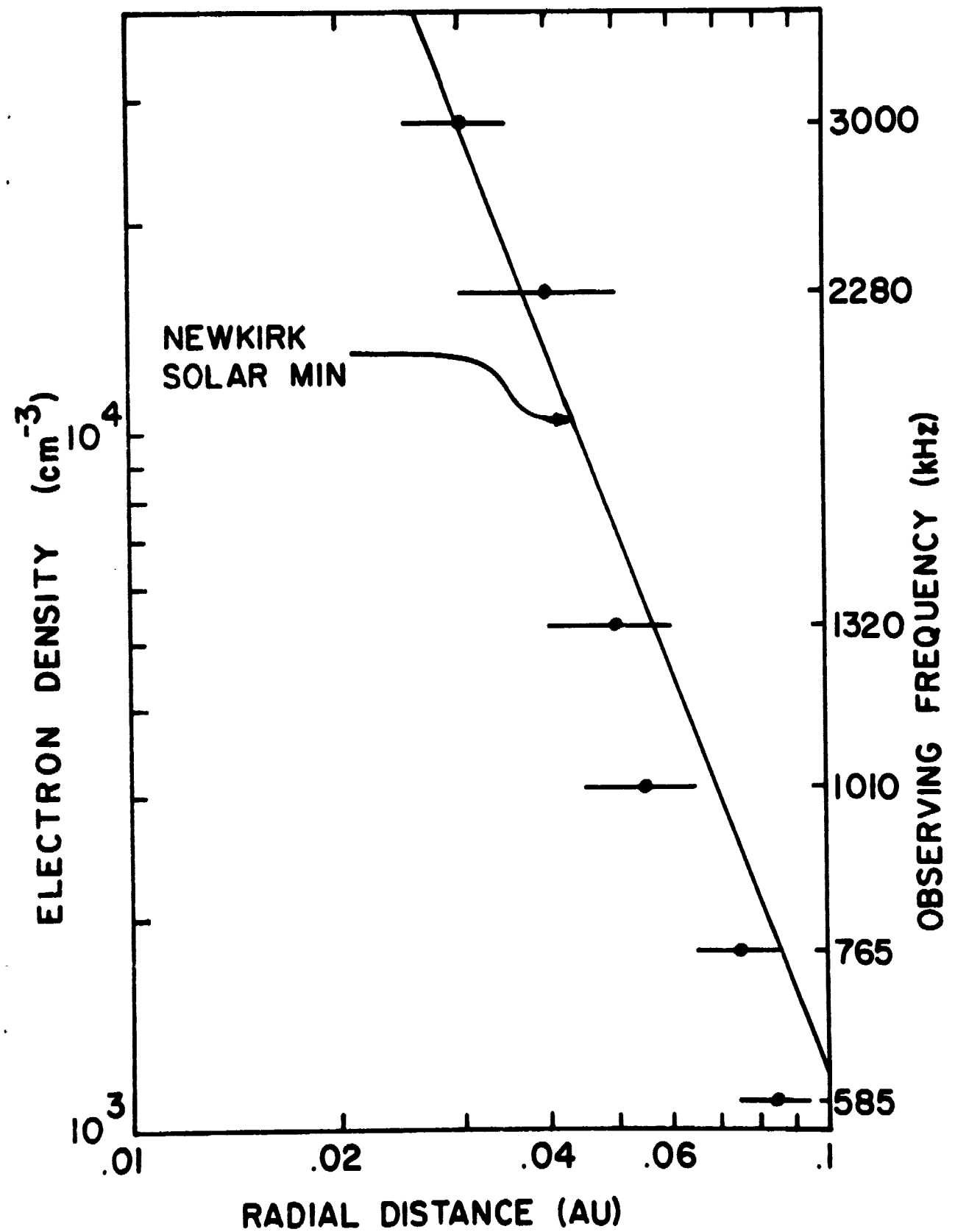
NEWKIRK
SOLAR MIN
ELECTRON DENSITY (cm^{-3})
10^4
10^3
3000
2280
1320
1010
765
585
OBSERVING FREQUENCY (kHz)
.01
.02
.04
.06
.1
RADIAL DISTANCE (AU)

Figure 5

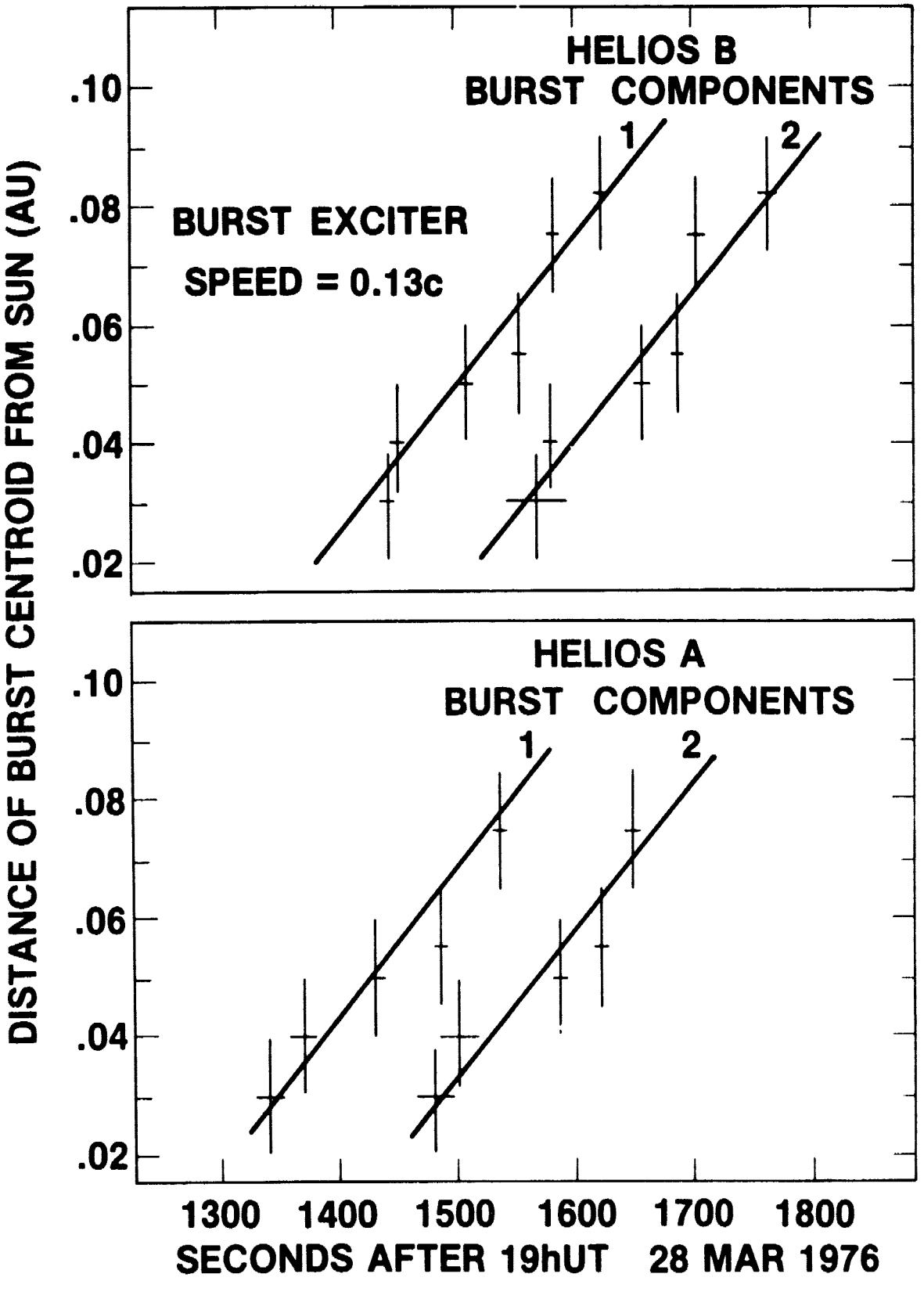
HELIOS B
BURST COMPONENTS
1
2
BURST EXCITER
SPEED = 0.13c
HELIOS A
BURST COMPONENTS
1
2
DISTANCE OF BURST CENTROID FROM SUN (AU)
.10
.08
.06
.04
.02
1300
1400
1500
1600
1700
1800
SECONDS AFTER 19hUT 28 MAR 1976

Figure 6

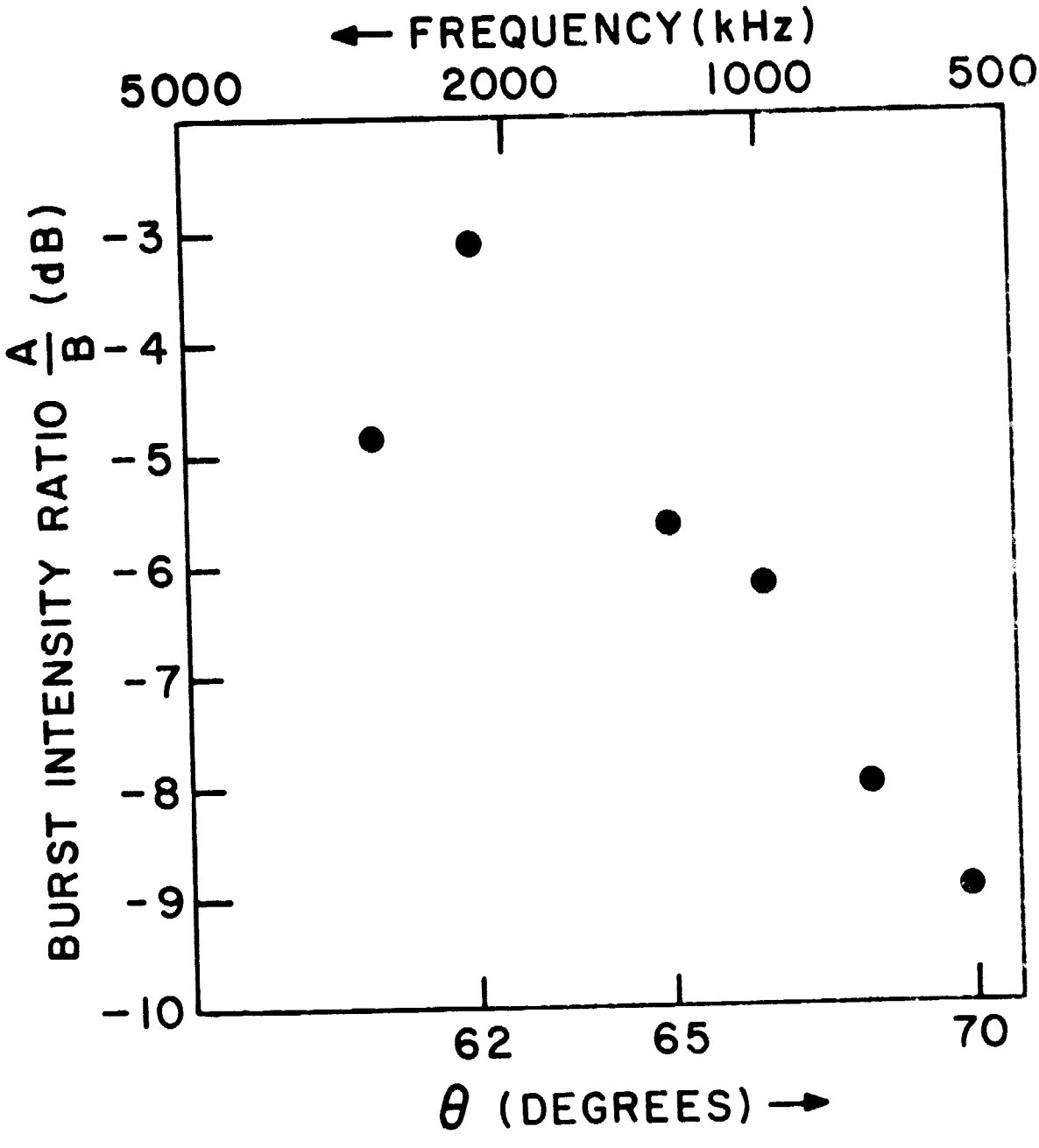
← FREQUENCY (kHz)
5000
2000
1000
500
BURST INTENSITY RATIO A/B (dB)
-3
-4
-5
-6
-7
-8
-9
-10
62
65
70
θ (DEGREES) →

Figure 7